Acta Cryst. (1999). B**55**, 1057–1067

TEMPO radicals showing magnetic interactions. II. 4-(Benzylideneamino)-TEMPO and related compounds

Fujiko Iwasaki,* Joseph H. Yoshikawa, Hajime Yamamoto, Kiwamu Takada, Eiji Kan-nari, Masanori Yasui, Takayuki Ishida and Takashi Nogami

Department of Applied Physics and Chemistry, The University of Electro-Communications, Chofu, Tokyo 182-8585, Japan. E-mail: fuji@pc.uec.ac.jp

(*Received 16 December 1998; accepted 26 May 1999*)

Abstract

X-ray crystal structure analyses were performed on 4-(Ar-methyleneamino)-TEMPO radicals at room temperature (TEMPO = 2,2,6,6-tetramethylpiperidyl-1-oxyl): Ar = Ph [4-(benzylideneamino)-2,2,6,6-tetramethylpiperidyl-1-oxyl], 4-MeS-Ph [2,2,6,6-tetramethyl-4-(4-methylthiobenzylideneamino)piperidyl-1-oxyl], 4-Me-Ph [4-(4-methylbenzylideneamino)-2,2,6,6-tetramethylpiperidyl-1-oxyl], 4-PhO-Ph [2,2,6,6-tetramethyl-4-(4-phenoxybenzylideneamino)piperidyl-1-oxyl], 4-$MeSO_2$-Ph [2,2,6,6-tetramethyl-4-(4-methylsulfonylbenzylideneamino)piperidyl-1-oxyl], 3-Py [2,2,6,6-tetramethyl-4-(3-pyridylmethylideneamino)piperidyl-1-oxyl] and 2-Naph [2,2,6,6-tetramethyl-4-(2-naphthylideneamino)piperidyl-1-oxyl]. Structures of Ph and 4-Me-Ph derivatives were also determined at 100 K. Some of these crystals have been revealed to show intermolecular ferromagnetic interactions at an extremely low temperature. Structural features of crystals of Ph, 4-MeS-Ph and 3-Py derivatives, which show ferromagnetic interactions, are very similar to each other. In these crystals, O atoms are arranged to form a sheet. The ferromagnetic interactions are considered to be transferred through O···H van der Waals' interactions of the β-H atoms of the neighboring TEMPO rings within the sheet. Between O···O sheets, the aryl groups are arranged in a herringbone manner. The crystal structure of the 4-Me-Ph derivative, which shows an antiferromagnetic interaction, is also pseudo-isostructural with those of Ph, 4-MeS-Ph and 3-Py derivatives, while the arrangement of the aryl groups is different. The packing mode of the crystals of the 4-$MeSO_2$-Ph derivative, of which the Weiss constant θ is nearly zero, is very different from those of the other derivatives showing magnetic interactions. The fact that the crystal structure of the paramagnetic 4-$MeSO_2$-Ph derivative does not show the O···O sheet structure accompanying the O···β-H interactions indicates that the intermolecular ferromagnetic interactions through β-H atoms within the O···O sheet are important for these TEMPO radical crystals.

1. Introduction

Some of the 4-arylmethyleneamino-TEMPO radicals (TEMPO = 2,2,6,6-tetramethylpiperidyl-1-oxyl) were

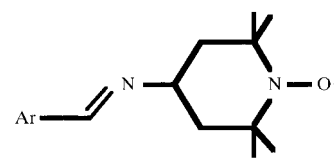

(1) Ar = 4-F-Ph
(2) Ar = 4-Cl-Ph
(3) Ar = 4-Br-Ph
(4) Ar = 4-I-Ph
(5) Ar = 4-Ph-Ph
(6) Ar = 4-Py
(7) Ar = 3,5-diCl-Ph
(8) Ar = Ph
(9) Ar = 4-MeS-Ph
(10) Ar = 3-Py
(11) Ar = 4-Me-Ph
(12) Ar = 2-Naph
(13) Ar = 4-PhO-Ph
(14) Ar = 4-$MeSO_2$-Ph

revealed to show intermolecular ferromagnetic interactions at an extremely low temperature (Ishida *et al.*, 1994; Ishida, Mitsubori *et al.*, 1995; Nogami *et al.*, 1994; Nogami *et al.*, 1995; Nogami, Ishida, Yasui, Iwasaki, Iwamura *et al.*, 1996; Togashi *et al.*, 1996). In the previous paper we reported the crystal structures of the 4-(4-halobenzylideneamino)-TEMPO radicals and related TEMPO radicals (Iwasaki *et al.*, 1999). These structural features were mainly classified into three groups

(i) crystal structures of (2) (Ar = 4-Cl-Ph), (4*a*) (Ar = 4-I-Ph) and (5) (Ar = 4-Ph-Ph), which show a ferromagnetic transition ($\theta > 0$ and $T_c > 0$),

(ii) structures of (3) (Ar = 4-Br-Ph) and (6) (Ar = 4-py) with ferromagnetic interactions ($\theta > 0$) and

(iii) others for antiferromagnetic (1) (Ar = 4-F-Ph) and (4*b*) (Ar = 4-I-Ph) ($\theta < 0$).

In these crystals, except (4*b*), sheet-like arrangements of the N—O radical groups and parallel overlaps of aryl groups between sheets were observed, which were considered to be major factors for the magnetic interactions. However, the X-ray crystal structure analyses revealed that there were other types of crystal structures of 4-Ar-CH═N-TEMPO radicals showing magnetic interactions: (8) (Ar = Ph, $T_c > 0$ K, $\theta > 0°$), (9) (Ar = 4-MeS-Ph, $T_c > 0$ K, $\theta > 0°$), (10) (Ar = 3-Py, $\theta > 0°$), (11) (Ar = 4-Me-Ph, $\theta < 0°$), (12) (Ar = 2-Naph) and (13)

Table 1. *Experimental details*

	(8*a*)	(8*b*)	(9)	(10)	(11*a*)
Crystal data					
Chemical formula	$C_{16}H_{23}N_2O$	$C_{16}H_{23}N_2O$	$C_{17}H_{25}N_2OS$	$C_{15}H_{22}N_3O$	$C_{17}H_{25}N_2O$
Chemical formula weight	259.37	259.37	305.46	260.36	273.40
Cell setting	Monoclinic	Monoclinic	Monoclinic	Monoclinic	Monoclinic
Space group	$P2_1/c$	$P2_1/c$	$P2_1/c$	$P2_1/c$	$P2_1/c$
a (Å)	12.684 (7)	12.5774 (14)	13.5737 (18)	12.425 (5)	12.490 (3)
b (Å)	11.740 (2)	11.6228 (16)	11.8796 (18)	11.598 (4)	11.597 (5)
c (Å)	11.024 (3)	10.8229 (17)	11.1628 (16)	11.038 (5)	11.280 (6)
β (°)	111.40 (4)	110.853 (9)	98.760 (11)	109.53 (4)	97.12 (3)
V (Å^3)	1528.3 (9)	1478.5 (3)	1779.0 (4)	1499.3 (10)	1621.3 (11)
Z	4	4	4	4	4
D_x (Mg m^{-3})	1.127	1.165	1.140	1.153	1.120
Radiation type	Mo $K\alpha$	Mo $K\alpha$	Mo $K\alpha$	Mo $K\alpha$	Mo $K\alpha$
Wavelength (Å)	0.71073	0.71073	0.71073	0.71073	0.71073
No. of reflections for cell parameters	25	25	25	25	25
θ range (°)	14.8–17.4	12.9–15.2	12.7–17.4	12.7–17.4	17.3–17.5
μ (mm^{-1})	0.071	0.073	0.183	0.074	0.070
Temperature (K)	296	100	296	297	294
Crystal form	Prism	Prism	Prism	Prism	Plate
Crystal size (mm)	0.50 × 0.40 × 0.20	0.35 × 0.35 × 0.20	0.50 × 0.35 × 0.25	0.20 × 0.20 × 0.20	0.40 × 0.40 ×0.10
Crystal color	Orange	Orange	Orange	Orange	Orange
Data collection					
Diffractometer	Rigaku AFC-7*R*	Rigaku AFC-7*R*	Rigaku AFC-7*R*	Rigaku AFC-5*R*	Rigaku AFC-7*R*
Data collection method	ω–2θ scans	ω–2θ scans	ω–2θ scans	ω–2θ scans	ω–2θ scans
Absorption correction	None	None	None	None	None
No. of measured reflections	3712	7062	4304	3608	3911
No. of independent reflections	3528	3383	4091	3432	3722
No. of observed reflections	2110	2731	2979	2096	2582
Criterion for observed reflections	$I > 2\sigma(I)$	$I > 2\sigma(I)$	$I > 2\sigma(I)$	$I > 2\sigma(I)$	$I > 2\sigma(I)$
R_{int}	0.0158	0.0230	0.0209	0.0201	0.0220
θ_{max} (°)	27.53	27.51	27.50	27.50	27.50
Range of h, k, l	$-16 \rightarrow h \rightarrow 15$ $-15 \rightarrow k \rightarrow 0$ $0 \rightarrow l \rightarrow 14$	$0 \rightarrow h \rightarrow 16$ $-15 \rightarrow k \rightarrow 15$ $-14 \rightarrow l \rightarrow 13$	$-17 \rightarrow h \rightarrow 17$ $-15 \rightarrow k \rightarrow 0$ $0 \rightarrow l \rightarrow 14$	$-16 \rightarrow h \rightarrow 15$ $0 \rightarrow k \rightarrow 15$ $0 \rightarrow l \rightarrow 14$	$-16 \rightarrow h \rightarrow 16$ $-15 \rightarrow k \rightarrow 0$ $0 \rightarrow l \rightarrow 14$
No. of standard reflections	3	3	3	3	3
Frequency of standard reflections	Every 150 reflections	Every 150 reflections	Every 150 reflections	Every 100 reflections	Every 150 reflections
Intensity decay (%)	7.23	0.527	0	0.046	2.41
Refinement					
Refinement on	F^2	F^2	F^2	F^2	F^2
$R[F^2>2\sigma(F^2)]$	0.0498	0.0358	0.0401	0.0488	0.0496
$wR(F^2)$	0.1470	0.0991	0.1217	0.1347	0.1617
S	1.012	1.016	1.015	0.981	1.036
No. of reflections used in refinement	3528	3383	4091	3432	3722
No. of parameters used	265	264	291	261	282
H-atom treatment	All H-atom parameters refined	All H-atom parameters refined	All H-atom parameters refined	All H-atom parameters refined	All H-atom parameters refined
Weighting scheme	$w = 1/[\sigma^2(F_o^2) + (0.0684P)^2 + 0.1077P]$, where $P = (F_o^2 + 2F_c^2)/3$	$w = 1/[\sigma^2(F_o^2) + (0.0459P)^2 + 0.3544P]$, where $P = (F_o^2 + 2F_c^2)/3$	$w = 1/[\sigma^2(F_o^2) + (0.0512P)^2 + 0.3325P]$, where $P = (F_o^2 + 2F_c^2)/3$	$w = 1/[\sigma^2(F_o^2) + (0.0580P)^2 + 0.2599P]$, where $P = (F_o^2 + 2F_c^2)/3$	$w = 1/[\sigma^2(F_o^2) + (0.0786P)^2 + 0.2899P]$, where $P = (F_o^2 + 2F_c^2)/3$
$(\Delta/\sigma)_{max}$	0.001	0.001	0.001	0.002	0.004

Table 1 (*cont.*)

	(8*a*)	(8*b*)	(9)	(10)	(11*a*)
$\Delta\rho_{max}$ (e Å^{-3})	0.170	0.268	0.227	0.149	0.203
$\Delta\rho_{min}$ (e Å^{-3})	−0.165	−0.184	−0.255	−0.120	−0.150
Extinction method	*SHELXL*97 (Sheldrick, 1997)	None	*SHELXL*97 (Sheldrick, 1997)	*SHELXL*97 (Sheldrick, 1997)	*SHELXL*97 (Sheldrick, 1997)
Extinction coefficient	0.021 (3)	0	0.0182 (16)	0.038 (3)	0.010 (2)
Source of atomic scattering factors	*International Tables for Crystallography* (1992, Vol. C, Tables 4.2.6.8 and 6.1.1.4)	*International Tables for Crystallography* (1992, Vol. C, Tables 4.2.6.8 and 6.1.1.4)	*International Tables for Crystallography* (1992, Vol. C, Tables 4.2.6.8 and 6.1.1.4)	*International Tables for Crystallography* (1992, Vol. C, Tables 4.2.6.8 and 6.1.1.4)	*International Tables for Crystallography* (1992, Vol. C, Tables 4.2.6.8 and 6.1.1.4)
Computer programs					
Data collection	*AFC* (Rigaku Co., 1994)	*AFC* (Rigaku Co., 1994)	*AFC* (Rigaku Co., 1994)	*AFC* (Rigaku Co., 1990)	*AFC* (Rigaku Co., 1994)
Cell refinement	*AFC* (Rigaku Co., 1994)	*AFC* (Rigaku Co., 1994)	*AFC* (Rigaku Co., 1994)	*AFC* (Rigaku Co., 1990)	*AFC* (Rigaku Co., 1994)
Data reduction	*TEXSAN* (MSC, 1992)	*TEXSAN* (MSC, 1992)	*TEXSAN* (MSC, 1992)	*TEXSAN* (MSC, 1992)	*TEXSAN* (MSC, 1992)
Structure solution	*SAPI*91 (Fan, 1991)	*SIR*88 (Burla *et al.*, 1989)	*SAPI*91 (Fan, 1991)	*SIR*88 (Burla *et al.*, 1989)	*SAPI*91 (Fan, 1991)
Structure refinement	*SHELXL*97 (Sheldrick, 1997)	*SHELXL*97 (Sheldrick, 1997)	*SHELXL*97 (Sheldrick, 1997)	*SHELXL*97 (Sheldrick, 1997)	*SHELXL*97 (Sheldrick, 1997)
Preparation of material for publication	*SHELXL*97 (Sheldrick, 1997)	*SHELXL*97 (Sheldrick, 1997)	*SHELXL*97 (Sheldrick, 1997)	*SHELXL*97 (Sheldrick, 1997)	*SHELXL*97 (Sheldrick, 1997)

	(11*b*)	(12)	(13)	(14)
Crystal data				
Chemical formula	$C_{17}H_{25}N_2O$	$C_{20}H_{25}N_2O$	$C_{22}H_{27}N_2O_2$	$C_{17}H_{25}N_2O_3S$
Chemical formula weight	273.40	309.43	351.47	337.46
Cell setting	Monoclinic	Orthorhombic	Orthorhombic	Monoclinic
Space group	$P2_1/c$	$Pna2_1$	$Pca2_1$	$P2_1/c$
a (Å)	12.4422 (19)	20.0837 (19)	30.565 (9)	11.1835 (18)
b (Å)	11.495 (3)	5.6969 (7)	5.993 (2)	15.487 (2)
c (Å)	11.094 (2)	15.106 (2)	22.032 (5)	11.5660 (18)
β (°)	97.381 (13)	90	90	114.539 (11)
V (Å^3)	1573.6 (5)	1728.4 (4)	4036 (2)	1822.2 (5)
Z	4	4	8	4
D_x (Mg m^{-3})	1.154	1.189	1.157	1.230
Radiation type	Mo $K\alpha$	Mo $K\alpha$	Mo $K\alpha$	Mo $K\alpha$
Wavelength (Å)	0.71073	0.71073	0.71073	0.71073
No. of reflections for cell parameters	24	25	25	24
θ range (°)	12.6–15.0	13.6–17.2	14.2–17.2	17.2–17.4
μ (mm^{-1})	0.072	0.073	0.074	0.193
Temperature (K)	100	295	297	294
Crystal form	Plate	Prism	Needle	Prism
Crystal size (mm)	0.40 × 0.40 × 0.10	0.50 × 0.38 × 0.10	0.70 × 0.50 × 0.40	0.40 × 0.40 × 0.25
Crystal color	Orange	Orange	Orange	Orange
Data collection				
Diffractometer	Rigaku AFC-7*R*	Rigaku AFC-5*R*	Rigaku AFC-4	Rigaku AFC-7*R*
Data collection method	ω–2θ scans	ω–2θ scans	ω–2θ scans	ω–2θ scans
Absorption correction	None	None	None	ψ scans (North *et al.*, 1968)
T_{min}	–	–	–	0.976
T_{max}	–	–	–	1.000
No. of measured reflections	3796	2059	4763	4390
No. of independent reflections	3611	2059	4763	4184
No. of observed reflections	2992	1491	2517	3223

Table 1 (*cont.*)

	(11*b*)	(12)	(13)	(14)
Criterion for observed reflections	$I > 2\sigma(I)$	$I > 2\sigma(I)$	$I > 2\sigma(I)$	$I > 2\sigma(I)$
R_{int}	0.0174	–	–	0.0114
θ_{max} (°)	27.50	27.48	27.49	27.50
Range of h, k, l	$-16 \rightarrow h \rightarrow 16$ $-14 \rightarrow k \rightarrow 0$ $0 \rightarrow l \rightarrow 14$	$0 \rightarrow h \rightarrow 26$ $0 \rightarrow k \rightarrow 7$ $0 \rightarrow l \rightarrow 19$	$0 \rightarrow h \rightarrow 39$ $0 \rightarrow k \rightarrow 7$ $-28 \rightarrow l \rightarrow 0$	$0 \rightarrow h \rightarrow 14$ $0 \rightarrow k \rightarrow 20$ $-15 \rightarrow l \rightarrow 13$
No. of standard reflections	3	3	3	3
Frequency of standard reflections	Every 150 reflections	Every 100 reflections	Every 50 reflections	Every 150 reflections
Intensity decay (%)	0.59	0.22	0	2.06
Refinement				
Refinement on	F^2	F^2	F^2	F^2
$R[F^2>2\sigma(F^2)]$	0.0551	0.0433	0.0588	0.0409
$wR(F^2)$	0.1653	0.1101	0.1242	0.1235
S	1.130	1.072	0.966	1.007
No. of reflections used in refinement	3611	2059	4763	4184
No. of parameters used	282	260	468	308
H-atom treatment	All H-atom parameters refined	Mixed	Mixed	All H-atom parameters refined
Weighting scheme	$w = 1/[\sigma^2(F_o^2) + (0.0592P)^2 + 1.6154P]$, where $P = (F_o^2 + 2F_c^2)/3$	$w = 1/[\sigma^2(F_o^2) + (0.0544P)^2 + 0.0293P]$, where $P = (F_o^2 + 2F_c^2)/3$	$w = 1/[\sigma^2(F_o^2) + (0.0471P)^2 + 0.0000P]$, where $P = (F_o^2 + 2F_c^2)/3$	$w = 1/[\sigma^2(F_o^2) + (0.0591P)^2 + 0.4517P]$, where $P = (F_o^2 + 2F_c^2)/3$
$(\Delta/\sigma)_{max}$	0.007	0.004	0.001	0.002
$\Delta\rho_{max}$ (e Å^{-3})	0.471	0.164	0.164	0.218
$\Delta\rho_{min}$ (e Å^{-3})	−0.306	−0.134	−0.162	−0.371
Extinction method	*SHELXL*97 (Sheldrick, 1997)	*SHELXL*97 (Sheldrick, 1997)	None	None
Extinction coefficient	0.007 (2)	0.017 (2)	–	–
Source of atomic scattering factors	*International Tables for Crystallography* (1992, Vol. C, Tables 4.2.6.8 and 6.1.1.4)	*International Tables for Crystallography* (1992, Vol. C, Tables 4.2.6.8 and 6.1.1.4)	*International Tables for Crystallography* (1992, Vol. C, Tables 4.2.6.8 and 6.1.1.4)	*International Tables for Crystallography* (1992, Vol. C, Tables 4.2.6.8 and 6.1.1.4)
Computer programs				
Data collection	*AFC* (Rigaku Co., 1994)	*AFC* (Rigaku Co., 1990)	*AFC* (Rigaku Co., 1978)	*AFC* (Rigaku Co., 1994)
Cell refinement	*AFC* (Rigaku Co., 1994)	*AFC* (Rigaku Co., 1990)	*AFC* (Rigaku Co., 1978)	*AFC* (Rigaku Co., 1994)
Data reduction	*TEXSAN* (MSC, 1992)	*TEXSAN* (MSC, 1992)	*TEXSAN* (MSC, 1992)	*TEXSAN* (MSC, 1992)
Structure solution	*SAPI*91 (Fan, 1991)	*SAPI*91 (Fan, 1991)	*SAPI*91 (Fan, 1991)	*SAPI*91 (Fan, 1991)
Structure refinement	*SHELXL*97 (Sheldrick, 1997)	*SHELXL*97 (Sheldrick, 1997)	*SHELXL*97 (Sheldrick, 1997)	*SHELXL*97 (Sheldrick, 1997)
Preparation of material for publication	*SHELXL*97 (Sheldrick, 1997)	*SHELXL*97 (Sheldrick, 1997)	*SHELXL*97 (Sheldrick, 1997)	*SHELXL*97 (Sheldrick, 1997)

(Ar = 4-PhO-Ph, $T_c > 0$ K, $\theta > 0°$). Structure analyses of (8) and (11) (100 K) were also carried out. The structure analysis of (14) (Ar = 4-$MeSO_2$-Ph) showing paramagnetic character ($\theta \simeq 0°$) was also carried out to compare the relationships between crystal structures and magnetic characters. Preliminary structures at room temperature have already been reported (Yasui *et al.*, 1996). In this paper we will report the detailed relationships between structural features and magnetic interactions of these crystals.

2. Experimental

Crystals of (8)–(14) for X-ray studies were grown from ethanol solutions. Crystal data, details concerning data collection and structure refinements are listed in Table 1.

Table 2. *Selected interatomic distances (Å) related to the O radical atoms of (8)–(11)*

Aryl group	(8*a*) Ph (296 K)	(8*b*) Ph (100 K)	(9) 4-MeS-Ph	(10) 3-Py	(11*a*) 4-Me-Ph (294 K)	(11*b*) 4-Me-Ph (100 K)
O1···O1^{i}	5.6173 (16)	5.5398 (9)	5.6688 (9)	5.591 (2)	5.688 (3)	5.6006 (11)
O1···O1^{ii}	6.1447 (13)	6.0841 (9)	6.2120 (12)	6.183 (2)	6.283 (2)	6.2237 (17)
O1···O1^{iii}				6.102 (3)		
O1···O1^{iv}					6.069 (3)	5.958 (3)
O1···C3^{ii}	3.378 (3)	3.3134 (14)	3.423 (2)	3.386 (2)	3.455 (2)	3.387 (3)
O1···C21^{ii}	3.429 (3)	3.3654 (16)	3.503 (3)	3.464 (3)	3.567 (3)	3.513 (3)
O1···H32^{ii}	2.50 (3)	2.422 (15)	2.59 (2)	2.49 (2)	2.56 (2)	2.50 (2)
O1···H22^{ii}	2.78 (3)	2.657 (16)	2.87 (3)	2.82 (2)	2.94 (3)	2.82 (3)
O1···H24^{i}	2.91 (3)	2.755 (15)	2.95 (3)	2.82 (2)		
O1···H31^{i}	3.172 (18)	3.028 (13)	3.220 (16)	2.99 (2)		
O1···H24^{v}					2.94 (3)	2.89 (2)
O1···H31^{v}					2.926 (18)	2.86 (3)

Symmetry codes: (i) $x, \frac{3}{2}-y, \frac{1}{2}+z$; (ii) $1-x, \frac{1}{2}+y, \frac{1}{2}-z$; (iii) $1-x, 2-y, 1-z$; (iv) $1-x, 2-y, -z$; (v) $x, \frac{3}{2}-y, -\frac{1}{2}+z$.

The intensity data were measured using Rigaku diffractometers AFC-4, AFC-5*R* or AFC-7*R* with a graphite monochromator.

The structures were solved by the direct method using the programs *SIR*88 (Burla *et al.*, 1989) and *SAPI*91 (Fan, 1991). Most of the H atoms were obtained from difference Fourier maps. The structures were refined by full-matrix least-squares with anisotropic temperature factors for non-H atoms and isotropic ones for H atoms, except (12) and (13). The coordinates of the H atoms of methyl groups of (12) and all H atoms of (13) are fixed during the refinements.†

3. Results and discussion

3.1. *Crystal structures*

The molecular structures along with the atomic numbering are shown in Fig. 1. For (8) and (11), no phase transitions were observed from room temperature to 100 K. The structural features of crystals of (8)–(11) are similar to each other, while the magnetic interaction of each radical is different. Stereoscopic views of these crystals are shown in Fig. 2.

The packing mode of (8) and (9) are very similar to each other, although the substituent (MeS group) of the aryl group of (9) is larger than that of (8) (H atom). These crystals show the ferromagnetic transition at extremely low temperatures. In these crystals, O atoms are arranged to form a zigzag sheet parallel to the *bc* plane. For (8) the nearest and second nearest O···O distances in the sheet are 5.6173 (16) and 6.1447 (13) Å, respectively, at room temperature. At 100 K these values reduce to 5.5398 (9) and 6.0841 (9) Å, respectively. Within the sheet, O atoms contact the H atoms of the CH_2 or CH_3 groups of the neighboring TEMPO rings with van der Waals distances, as shown in Table 2 and Fig. 3. The ferromagnetic interactions are considered to be transferred through O···H van der Waals interac-

Table 3. *Selected intermolecular distances (Å) related to the O atoms of (12) and (13)*

Aryl group	(12) 2-Naph
O1···O1^{i}	5.6969 (7)
O1···O1^{ii}	8.748 (3)
O1···C4^{i}	3.580 (4)
O1···C12^{iii}	3.477 (4)
O1···C17^{iii}	3.483 (4)
O1···C22^{i}	3.705 (4)
O1···C61^{i}	3.772 (5)
O1···H4^{i}	2.56 (3)
O1···H25^{i}	2.78 (2)
O1···H62^{i}	2.87 (2)
O1···H12^{iii}	2.75 (3)
O1···H17^{iii}	2.80 (4)

Symmetry codes: (i) $x, y-1, z$; (ii) $-x, -y-1, \frac{1}{2}+z$; (iii) $-x, -y, \frac{1}{2}+z$.

Aryl group	(13) 4-PhO-Ph
O1*A*···O1*B*	7.998 (5)
O1*A*···O1*A*^{i}	5.993(2)
O1*B*···O1*B*^{i}	5.993 (2)
O1*A*···O1*B*^{ii}	8.033 (5)
O1*A*···C22*A*^{i}	3.695 (6)
O1*B*···C61*B*^{i}	3.862 (6)
O1*A*···C46*B*^{iii}	3.189 (5)
O1*B*···C46*A*^{iv}	3.361 (5)
O1*A*···H25*A*^{i}	2.67
O1*B*···H62*B*^{i}	2.83
O1*A*···H46*B*^{iii}	2.45
O1*B*···H46*A*^{iv}	2.74
O2*A*···C45*A*^{i}	3.344 (6)
O2*B*···C45*B*^{i}	3.307 (6)
O2*B*···C44*B*^{i}	3.325 (6)

Symmetry codes: (i) $x, 1+y, z$; (ii) $\frac{1}{2}+x, 3-y, z$; (iii) $\frac{1}{2}-x, 1+y, \frac{1}{2}+z$; (iv) $\frac{1}{2}-x, 2+y, \frac{1}{2}+z$.

† Supplementary data for this paper are available from the IUCr electronic archives (Reference: OA0021). Services for accessing these data are described at the back of the journal.

tions of these β-H atoms, as in the case of 4-Cl-Ph (2), 4-Br-Ph (3) and 4-I-Ph (4*a*) derivatives, which also show ferromagnetic interactions (Nogami *et al.*, 1995; Nogami, Ishida, Yasui, Iwasaki, Iwamura *et al.*, 1996; Nogami, Ishida, Yasui, Iwasaki, Takeda *et al.*, 1996; Iwasaki *et al.*, 1999). Between sheets, the aryl groups related by 2_1 symmetry are arranged in a herringbone manner, while the aryl groups of (2), (3) and (4*a*) stack alternately, face-to-face by the center of symmetry. In the case of (8) and (9), as well as (10), there are no contacts between the aryl groups related by the center of symmetry.

The crystals of (10) are pseudoisostructural to (8) and (9). The arrangement of the molecules within the O···O sheet is very similar to those of (8) and (9), although the intersheet aryl–aryl relation related by the 2_1 axis is different from those of (8) and (9). The dihedral angles of aryl planes related by the 2_1 axis are 31.56 (6), 33.51 (3), 37.49 (5), 10.55 (7), 1.94 (12) and 1.87 (12)° for (8*a*), (8*b*) (100 K), (9), (10), (11*a*) and (11*b*) (100 K), respectively.

The crystals of (11) are also pseudoisostructural to those of (8)–(10), if the unit cell of (11) is converted to

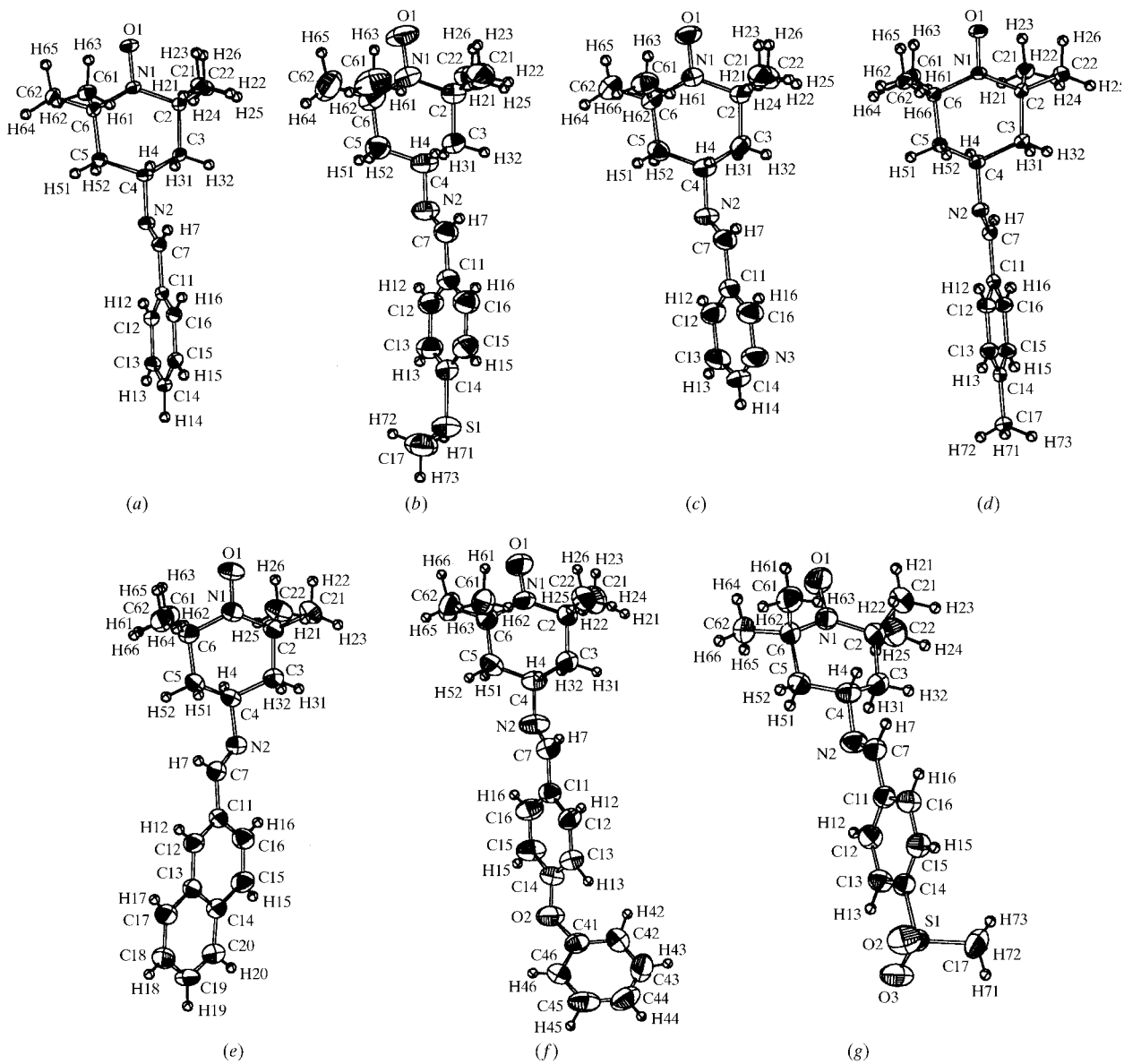

Fig. 1. *ORTEP* (Johnson, 1976) drawings of the molecules with atom numbering. The thermal ellipsoids for non-H atoms are drawn at 50% probability and the H atoms are drawn as spheres with a radius of 0.1 Å. (*a*) (8*b*) Ph (100 K), (*b*) (9) 4-MeS-Ph, (*c*) (10) 3-Py, (*d*) (11*b*) 4-Me-Ph (100 K), (*e*) (12) 2-Naph, (*f*) (13*a*) 4-PhO-Ph (molecule *A*) and (*g*) (14) 4-$MeSO_2$-Ph.

$a' = -a$, $b' = -b$, $c' = c$ and $\beta' = 90 - \beta$ and atomic parameters are transformed to $x' = x$, $y' = y$ and $z' = \frac{1}{2} - z$. Atomic coordinates of x and y (and also x' and y') are very close to those of (8)–(10), while z' parameters are shifted from the corresponding parameters of (8)–(10) by ~0.1. The relationship between TEMPO rings in the unit cell is similar to those of (8)–(10), so the structural feature within the O···O sheet of (11) is very similar to those of (8)–(10). The O···O sheet structures and the contacts with β-H atoms, which are characteristic for the ferromagnetic interactions, are also observed in (11), which shows the antiferromagnetic interaction. On the other hand, the intersheet arrangement of aryl rings of (11) is different from those of (8)–(10), because of the total shift of the molecule along the c axis. In (11) aryl groups related by the center of symmetry, not by the 2_1 symmetry, are arranged side-by-side, as shown in Fig. 2. These aryl groups are not stacked in a face-to-face manner, whereas in (2), (3) and (4*a*) the aryl groups related by the center of symmetry stack alternately in a face-to-face manner.

In the crystals of the TEMPO radicals (2), (3), (4*a*), (5), (6), (8), (9) and (10), showing ferromagnetic interactions, the O···O sheet structures and the intrasheet O···β-H contacts are observed, although the packing modes of (2), (3), (4*a*), (5) and (6) are quite different from those of (8)–(10). The ferromagnetic interactions are considered to be transferred through O···β-H van der Waals interactions, as mentioned previously. In the case of the crystals of (1), showing an antiferromagnetic interaction, the intrasheet O···γ-H contact is observed, which is considered to cause the antiferromagnetic interaction. In the case of (11), which also shows an antiferromagnetic interaction, the intrasheet arrangement is very similar to those of (8)–(10) and no intrasheet O···γ-H contact is observed. The difference in the arrangement of the aryl groups between (8)–(10) and (11) may be considered to cause the different magnetic properties.

It is interesting that the crystal structure of the 4-Me-Ph derivative (11) is quite different from those of 4-Cl-Ph (2) and 4-Br-Ph (3) derivatives, although the shape and size of a molecule of (11) are very similar to those of (2) and (3). In these crystals the packing may be ruled by the aryl groups having different kinds of electronic properties.

The crystal structure of (12) is shown in Fig. 4. The selected intermolecular distances are listed in Table 3. The nearest O1···O1^{i} [(i) $x, y-1, z$] contact is 5.6969 (7), which corresponds to the length of the b axis. The second nearest O1···O1^{ii} [(ii) $-x, -y-1, \frac{1}{2}+z$] distance is 8.748 (3) Å. The pleated sheet is formed

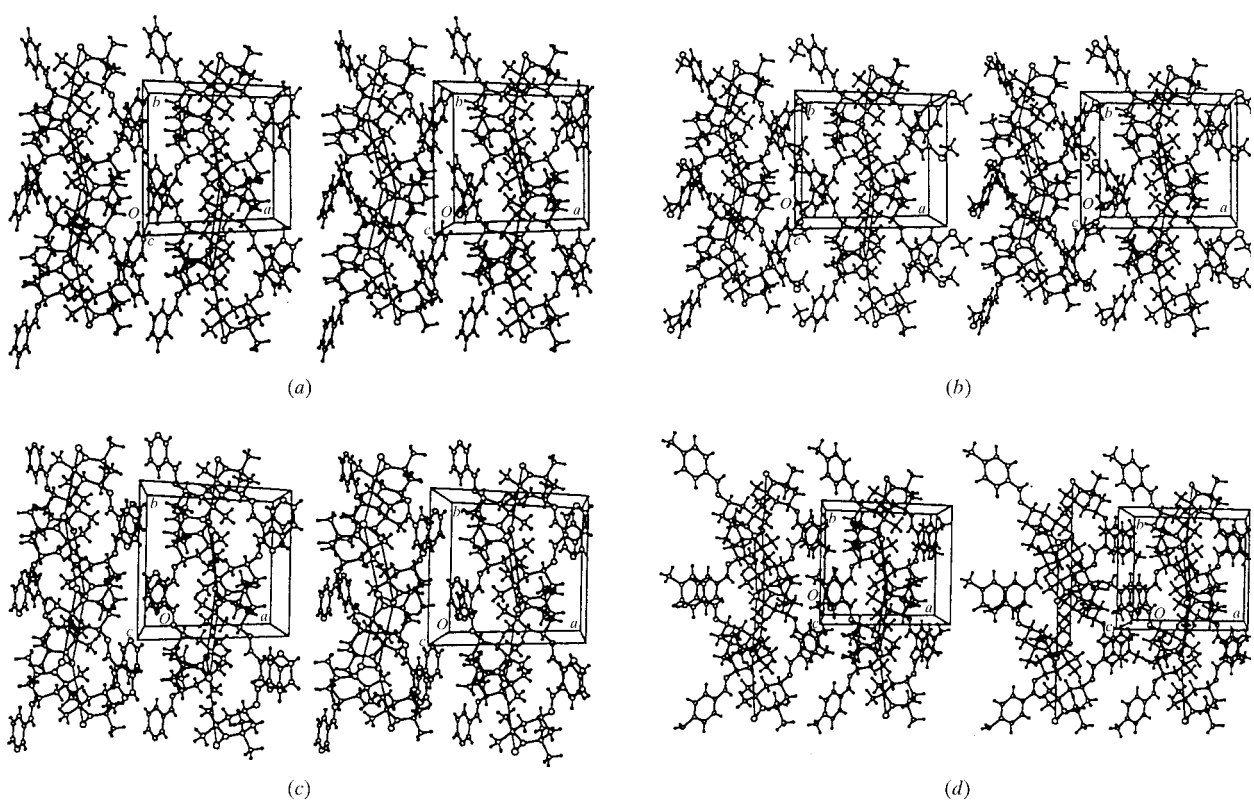

Fig. 2. Stereoscopic views of the crystal structures. (*a*) (8) Ph, (*b*) (9) 4-MeS-Ph, (*c*) (10) 3-Py and (*d*) (11) 4-Me-Ph.

parallel to the *bc* plane. Within the sheet the contacts are observed between O1 and β-H atoms (H25^{i} and H62^{i}) and also the γ-H atom (H4^{i}), as shown in Table 3. There are no direct O···H contacts between O1 and O1^{ii}. The van der Waals contacts are observed between O1 and H12^{iii} and H17^{iii} [(iii) $-x, -y, \frac{1}{2}+z$] of the naphthyl group. Between sheets the aryl groups are arranged in an approximate herringbone. In the case of (12) metamagnetic character has been shown at extremely low temperature, while a positive Weiss constant was observed (Ishida, Tomioka *et al.*, 1995). An origin of the antiferromagnetic interaction may occur from the O···O contact through the γ-H atom.

The crystal structure of (13) is quite different from the other derivatives, as shown in Fig. 5. There are two independent molecules (*A* and *B*) in an asymmetric unit. The relationship between *A* and *B* is $x_A - x_B = 0.25$, $y_A - y_B = -0.42$ and $z_A - z_B = 0.00$, which is a simple translation. To apply the crystallographic symmetry operation the local glide planes can be generated between the molecule *A* and *B*. An O···O network plane is formed perpendicular to the *c* axis. The distances of O···O contacts are 5.993 (2) for O1*A*···O1*A*^{i} and O1*B*···O1*B*^{i} [(i) $x, y+1, z$], and 7.998 (5) Å for O1*A*···O1*B* and 8.033 (5) Å for O1*A*···O1*B*^{ii} [(ii) $\frac{1}{2}+x, 3-y, z$], as shown in Table 3. Radical O atoms O1*A* and O1*B* contact to β-H atoms H25*A*^{i} and H62*B*^{i}, respectively, with the van der Waals contact. Between sheets, aryl groups belonging to the one side of the sheets are arranged. Therefore, no face-to-face overlaps or herringbone arrangements of aryl

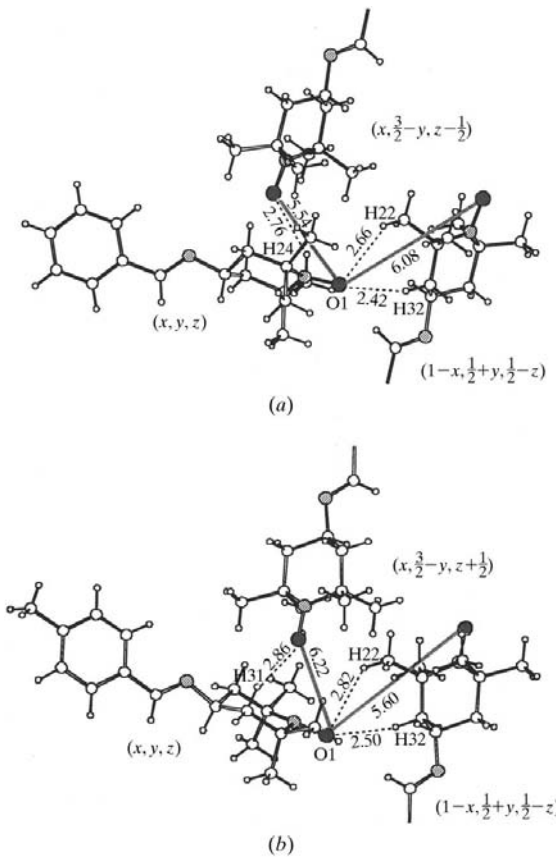

Fig. 3. Perspective views of the intermolecular relationships between O and β-H atoms at 100 K. (*a*) (8*b*) Ph and (*b*) (11*b*) 4-Me-Ph.

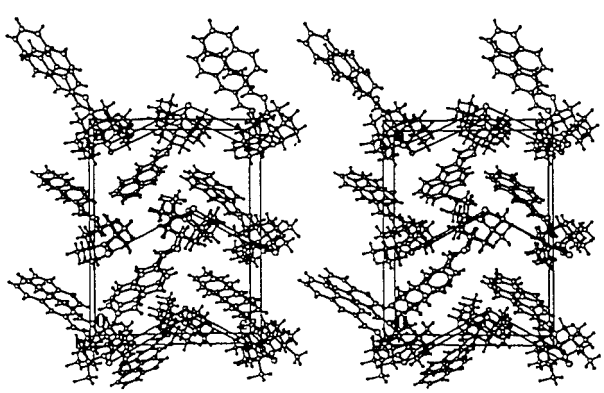

Fig. 4. Stereoscopic view of the crystal structure of (12) 2-Naph.

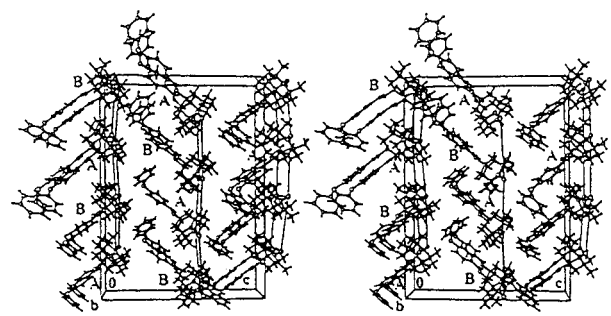

Fig. 5. Stereoscopic view of the crystal structure of (13) 4-PhO-Ph.

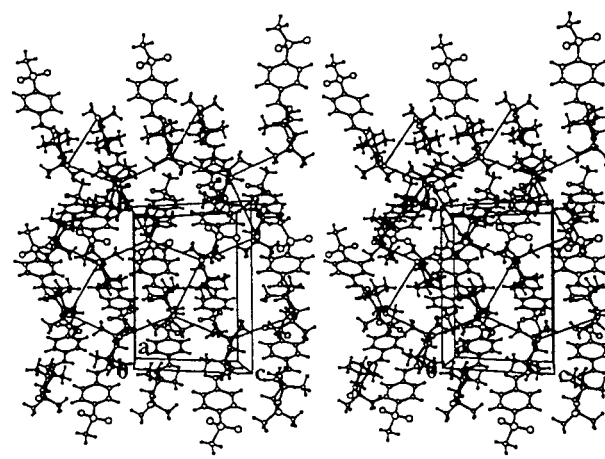

Fig. 6. Stereoscopic view of the crystal structure of (14) 4-MeSO$_2$-Ph.

Table 4. *Selected geometric parameters (Å, °)*

	(8*a*)	(8*b*)	(9)	(10)	(11*a*)	(11*b*)	(12)	(13*A*)	(13*B*)	(14)
Aryl group	Ph	Ph	4-MeS-Ph	3-Py	4-Me-Ph	4-Me-Ph	2-Naph	4-PhO-Ph		4-MeSO$_2$-Ph
Temperature (K)	296	100	296	297	294	100	295	297		294
Weiss constant (K)	0.7	0.7	0.5	0.4	−1.3	−1.3	0.3	0.4		0.06
Magnetic tranistion point (K)	0.3	0.3						0.2		
O1—N1	1.2818 (18)	1.2888 (11)	1.2845 (16)	1.2839 (17)	1.2846 (16)	1.2881 (19)	1.286 (3)	1.270 (4)	1.260 (4)	1.2832 (17)
N1—C2	1.492 (2)	1.4988 (14)	1.488 (2)	1.491 (2)	1.494 (2)	1.496 (2)	1.491 (4)	1.486 (5)	1.502 (5)	1.489 (2)
N1—C6	1.492 (2)	1.4941 (13)	1.487 (2)	1.492 (2)	1.488 (2)	1.498 (2)	1.497 (4)	1.507 (5)	1.501 (5)	1.496 (2)
N2—C4	1.466 (2)	1.4683 (13)	1.4687 (18)	1.469 (2)	1.4690 (19)	1.463 (2)	1.480 (4)	1.464 (5)	1.462 (5)	1.470 (2)
N2—C7	1.254 (2)	1.2659 (14)	1.251 (2)	1.241 (2)	1.251 (2)	1.267 (3)	1.262 (4)	1.246 (5)	1.268 (4)	1.254 (2)
C2—C3	1.528 (2)	1.5341 (14)	1.529 (2)	1.528 (2)	1.531 (2)	1.526 (2)	1.530 (4)	1.531 (5)	1.538 (5)	1.528 (2)
C3—C4	1.512 (3)	1.5247 (15)	1.506 (2)	1.516 (3)	1.513 (2)	1.530 (3)	1.521 (4)	1.501 (5)	1.520 (5)	1.515 (2)
C4—C5	1.517 (3)	1.5228 (15)	1.517 (2)	1.513 (3)	1.517 (2)	1.526 (3)	1.518 (4)	1.513 (5)	1.510 (5)	1.516 (3)
C5—C6	1.523 (2)	1.5314 (14)	1.527 (2)	1.524 (2)	1.531 (2)	1.526 (2)	1.538 (4)	1.533 (6)	1.521 (6)	1.525 (2)
C7—C11	1.475 (2)	1.4779 (14)	1.472 (2)	1.473 (2)	1.474 (2)	1.469 (2)	1.466 (4)	1.488 (5)	1.473 (5)	1.474 (2)
O1—N1—C2—C3	−169.38 (15)	−170.02 (9)	−169.95 (15)	−169.04 (14)	168.74 (13)	168.89 (14)	168.0 (2)	−158.2 (3)	−161.7 (3)	−166.73 (16)
O1—N1—C6—C5	169.01 (15)	169.67 (8)	169.16 (14)	169.11 (14)	−167.92 (13)	−168.33 (15)	−167.4 (3)	158.7 (3)	162.0 (3)	165.91 (16)
C6—N1—C2—C3	34.6 (2)	35.14 (13)	32.6 (2)	36.4 (2)	−36.5 (2)	−37.3 (2)	−33.8 (4)	42.2 (5)	43.1 (5)	34.7 (2)
C2—N1—C6—C5	−34.9 (2)	−35.36 (13)	−33.3 (2)	−36.2 (2)	37.34 (19)	37.8 (2)	34.2 (4)	−41.3 (5)	−42.6 (5)	−35.6 (2)
N1—C2—C3—C4	−45.5 (2)	−45.73 (12)	−44.4 (2)	−45.6 (2)	45.18 (19)	45.9 (2)	45.7 (3)	−46.9 (5)	−48.6 (4)	−45.9 (2)
N1—C6—C5—C4	45.9 (2)	46.37 (12)	45.7 (2)	45.6 (2)	−47.24 (19)	−47.5 (2)	−47.2 (4)	44.9 (5)	47.0 (5)	47.6 (2)
C2—C3—C4—C5	59.2 (2)	59.46 (11)	59.37 (18)	57.4 (2)	−57.23 (18)	−57.4 (2)	−61.3 (3)	54.7 (5)	56.5 (4)	60.9 (2)
C3—C4—C5—C6	−59.6 (2)	−59.89 (11)	−60.16 (18)	−57.7 (2)	58.65 (18)	58.64 (19)	62.5 (4)	−54.0 (5)	−55.3 (4)	−62.0 (2)
N2—C4—C3—C2	177.30 (15)	177.14 (8)	177.13 (14)	175.29 (14)	−174.51 (13)	−174.61 (15)	171.4 (3)	171.1 (3)	172.8 (3)	179.57 (15)
N2—C4—C5—C6	−178.13 (15)	−177.95 (9)	−178.61 (14)	−175.87 (15)	176.72 (13)	176.46 (14)	−174.9 (3)	−171.2 (3)	−171.1 (3)	179.67 (15)
C7—N2—C4—C3	109.92 (19)	112.82 (11)	108.56 (17)	102.9 (2)	−100.27 (18)	−98.95 (19)	112.6 (3)	107.0 (5)	114.0 (4)	109.25 (19)
C7—N2—C4—C5	−132.12 (18)	−129.47 (10)	−133.75 (16)	−138.93 (18)	142.12 (16)	143.65 (17)	−9.4 (4)	−134.1 (4)	−128.3 (4)	−133.05 (18)

groups are observed. In the crystals of (2)–(6) in the previous paper (Iwasaki *et al.*, 1999) and (8)–(12) in the present paper, [O···O sheet]-Ar···Ar-[O···O sheet]-Ar arrangements are characteristic features of the crystal structures, while in (13) the motif of the structure is [O···O sheet]-Ar···[O···O sheet]-Ar. O1*A* and O1*B* atoms also contact to H atoms of phenoxy groups.

A stereoscopic view of the structure of (14) is depicted in Fig. 6. The packing mode of (14), of which θ is nearly zero, is very different from those of the other derivatives showing magnetic interactions. The contacts between radical O atoms are 6.199 (1) and 6.764 (3) Å for O1···O1^{i} [(i) $x, -\frac{1}{2}-y, \frac{1}{2}+z$] and O1···O1^{ii} [(ii) $-1-x, -y, -z$], respectively. Zigzag O···O chains formed by the *c*-glide symmetry are linked by the O···O contacts formed by the center of symmetry. The O···O arrangement is not a sheet as shown in Fig. 6. In this case there are no van der Waals contacts between the radical O atom O1 and the β-H atoms of the neighboring TEMPO rings. Slightly short contacts are observed between O atoms of the sulfonyl group and H atoms of the neighboring molecules: 2.47 (2) Å for O3···H15^{iii} [(iii) $x, \frac{1}{2}-y, -\frac{1}{2}+z$] and 2.69 (2) Å for O2···H63^{iv} [(iv) $1-x, -y, 1-z$]. The fact that the crystal structure of paramagnetic (14) does not show the O···O sheet structure accompanying the O···β-H interactions demonstrates that the intermolecular ferromagnetic interactions through the β-H atoms within the O···O sheet is important for these TEMPO radicals.

3.2. *Molecular structures*

Selected bond lengths and torsion angles are listed in Table 4. A conformation of the TEMPO ring of each derivative is a shallow chair form. The torsion angles within the rings are C—C—N1—C ±32.6 (2) to ±37.8 (2), N1—C—C—C ±44.4 (2) to ±47.6 (2) and C—C—C—C ±57.2 (2) to ±62.5 (2)° for (8)–(12) and (14). For (13) the mean absolute values of the corresponding angles are 42.3 (5), 46.8 (5) and 55.1 (5)° for C—C—N1—C, N1—C—C—C and C—C—C—C, respectively. The exocyclic torsion angles C3—C4—N2—C7 and C5—C4—N2—C7 of (10) and (11) are different from those of (8), (9), (13) and (14) by ∼5–6°. The difference of these exocyclic torsion angles between (8), (9) and (10), (11) is related to the crystal packing, that is, the difference of the dihedral angles of the aryl groups related by the 2_1 symmetry. The absolute values of the torsion angles of N2—C4—C—C of (8) and (9) showing a ferromagnetic transition are larger than those of (2), (4*a*) and (5), which also show a ferromagnetic transition, by ∼5–6°. These differences of torsion angles correspond to the types of crystal structure. Recently we performed the structure analyses of mixed crystals of (2) and (3), and those of (2) and (11). The preliminaly result showed that the crystal structures of the mixed crystals are isomorphous to those of either components, and both of the crystal forms of components were observed. The molecules are disordered only at the substituents, but the other moieties are ordered. The observed conformations of the component molecules depend on the crystal forms of the mixed crystals (Hashizume *et al.*, 1999).

The torsion angles of C—C4—N2—C7 of (12) are quite different from the other molecules. The reason for the difference may be caused from the packing effect of the large and rigid naphthyl groups between the sheets.

For all molecules except (13), the distances of O1—N1 are very similar to those of 4-halophenyl derivatives. For (13) the corresponding values are slightly shorter than the others by 0.02 Å. The bond lengths of N2—C4 of (8)–(11) [1.462 (5)–1.469 (2) Å] are slightly shorter than the corresponding lengths of (2)–(5) [1.470 (3)–1.479 (4) Å]. The bond lengths of (8*b*) and (11*b*) at 100 K are longer than those of the corresponding lengths of (8*a*) and (11*a*) at room temperature, which is due to the decreasing of the thermal motion. The fact that the corresponding bond lengths and angles of the ferromagnetic (8*b*) and the antiferromagnetic (11*b*) are very similar to each other indicates little, if any, relation between the molecular structures and the magnetic interactions.

In the crystals of TEMPO radicals, the sheet-like arrangements of O atoms and intrasheet interactions through β-H atoms of the CH_2 or CH_3 groups of the neighboring TEMPO rings are related to the mechanisms of the ferromagnetic interactions, although various types of the arrangements of aryl groups are observed. In the case of the antiferromagnetic 4-F-Ph derivative (1) and metamagnetic 2-Naph derivative (12), intrasheet interactions through the γ-H atom were observed. The fact that no sheet structure was observed in the crystals of the paramagnetic 4-MeSO_2-Ph derivative (14) confirms the relationships between O···O sheet structures and magnetic interactions.

This work was supported in part by a Grant-in-Aid for Scientific Research (No. 08454180) from the Ministry of Education, Science and Culture.

References

Burla, M. C., Camalli, M., Cascarano, G., Giacovazzo, C., Polidori, G., Spagna, R. & Viterbo, D. (1989). *J. Appl. Cryst.* **22**, 389–393.

Fan, H.-F. (1991). *SAPI*91. *Structure Analysis Programs with Intelligent Control.* Tokyo, Japan: Rigaku Co.

Hashizume, D., Takashima, N., Miki, R., Yasui, M. & Iwasaki, F. (1999). To be published.

Ishida, T., Mitsubori, S., Nogami, T., Ishikawa, Y., Yasui, M., Iwasaki, F., Iwamura, H., Takeda, N. & Ishikawa, M. (1995). *Syn. Met.* **71**, 1791–1792.

Ishida, T., Tomioka, K., Nogami, T., Yoshikawa, H., Yasui, M., Iwasaki, F., Takeda, N. & Ishikawa, M. (1995). *Chem. Phys. Lett.* **247**, 7–12.

Ishida, T., Tsuboi, H., Nogami, T., Yoshikawa, H., Yasui, M., Iwasaki, F., Iwamura, H., Takeda, N. & Ishikawa, M. (1994). *Chem. Lett.* pp. 919–922.

Iwasaki, F., Yoshikawa, J. H., Yamamoto, H., Takada, K., Kannari, E., Yasui, M., Ishida, T. & Nogami, T. (1999). *Acta Cryst.* B**55**, 231–245.

Johnson, C. K. (1976). *ORTEP*II. Report ORNL-5138. Oak Ridge National Laboratory, Tennessee, USA.

Molecular Structure Corpration (1992). *TEXSAN. Crystal Structure Analysis Package.* MSC, 3200 Research Forest Drive, The Woodlands, TX 77381, USA.

Nogami, T., Ishida, T., Tsuboi, H., Yoshikawa, H., Yamamoto, H., Yasui, M., Iwasaki, F., Iwamura, H., Takeda, N. & Ishikawa, M. (1995). *Chem. Lett.* pp. 635–636.

Nogami, T., Ishida, T., Yasui, M., Iwasaki, F., Iwamura, H., Takeda, N. & Ishikawa, M. (1996). *Mol. Cryst. Liq. Cryst.* **279**, 97–106.

Nogami, T., Ishida, T., Yasui, M., Iwasaki, F., Takeda, N., Ishikawa, M., Kawakami, T. & Yamaguchi, K. (1996). *Bull. Chem. Soc. Jpn*, **69**, 1841–1848.

Nogami, T., Tomioka, K., Ishida, T., Yoshikawa, H., Yasui, M., Iwasaki, F., Iwamura, H., Takeda, N. & Ishikawa, M. (1994). *Chem. Lett.* pp. 29–32.

North, A. C. T., Phillips, D. C. & Mathews, F. S. (1968). *Acta Cryst.* A**24**, 351–359.

Rigaku Corporation (1978). *AFC. Diffractometer Control Software*. Rigaku Corporation, Tokyo, Japan.

Rigaku Corporation (1990). *AFC. Diffractometer Control Software*. Rigaku Corporation, Tokyo, Japan.

Rigaku Corporation (1994). *AFC. Diffractometer Control Software*. Rigaku Corporation, Tokyo, Japan.

Sheldrick, G. M. (1997). *SHELXL*97. *Program for Crystal Structure Determination.* University of Göttingen, Germany.

Togashi, K., Imachi, R., Tomioka, K., Tuboi, H., Ishida, T., Nogami, T., Takeda, N. & Ishikawa, M. (1996). *Bull. Chem. Soc. Jpn*, **69**, 2821–2830.

Yasui, M., Yoshikawa, H., Yamamoto, H., Ishida, T., Nogami, T. & Iwasaki, F. (1996). *Mol. Cryst. Liq. Cryst.* **279**, 77–85.